may exist that monitor histone acetylation or higher order chromatin structure. It should now be possible to study the regulation of histone deacetylase during the cell cycle, its substrate specificity, and the mechanism by which it is targeted to specific regions of the genome.

REFERENCES AND NOTES

1. B. M. Turner, *Cell* **75**, 5 (1993).
2. D. Y. Lee, J. J. Hayes, D. Pruss, A. P. Wolffe, *ibid.* **72**, 73 (1993).
3. S. Kleff, E. D. Andrulis, C. W. Anderson, R. Sternglanz, *J. Biol. Chem.* **270**, 24674 (1995).
4. M. Yoshida, S. Horinouchi, T. Beppu, *Bioessays* **17**, 423 (1995).
5. M. Kijima, M. Yoshida, K. Sugita, S. Horinouchi, T. Beppu, *J. Biol. Chem.* **268**, 22429 (1993).
6. J. Taunton, J. L. Collins, S. L. Schreiber, in preparation.
7. All procedures were done at 4°C. Thymocytes (~12 g) prepared from fresh bovine thymus were homogenized in hypotonic lysis buffer [20 mM tris (pH 7.8), 20 mM NaCl, 1 mM EDTA, 10% glycerol, 1 mM phenylmethylsulfonyl fluoride, 1 mM benzamidine, and 10 μg/ml each of pepstatin, aprotinin, and leupeptin] by mechanical disruption, and the nuclei were isolated by centrifugation at 3000*g*. Nuclei were resuspended in lysis buffer, and the proteins were extracted with 0.4 M ammonium sulfate. The viscous lysate was sonicated and clarified by centrifugation at 100,000*g* for 1 hour. Proteins were then precipitated with 90% saturated ammonium sulfate and recovered by centrifugation (100,000*g* for 1 hour). After thorough dialysis against Q buffer (25 mM tris, pH 8, 10 mM NH_4Cl, 0.25 mM EDTA, and 10% glycerol), a portion of the nuclear proteins (~12 mg of total protein) was loaded onto an HR 10/10 MonoQ column (Pharmacia). The column was washed with 25 ml of Q buffer and eluted with a 50-ml linear gradient of 10 to 500 mM NH_4Cl. The column was further washed with 25 ml of 500 mM NH_4Cl and 25 ml of 1 M NH_4Cl. Fractions (2.5 ml) were then analyzed for trapoxin binding and histone deacetylase activities or further purified with the K-trap affinity matrix.
8. J. Taunton, C. A. Hassig, S. L. Schreiber, unpublished results.
9. In vitro binding experiments with soluble [^{3}H]trapoxin indicated that the radiolabel is released into solution after protein denaturation with SDS or guanidinium hydrochloride. Thus, trapoxin binding proteins were expected to elute from the affinity matrix with SDS (J. Taunton, C. A. Hassig, S. L. Schreiber, unpublished observations).
10. To obtain enough trapoxin binding protein for microsequencing, we prepared nuclear ammonium sulfate pellets from 15 bovine thymuses as described (*7*). Sedimented proteins were resuspended in and dialyzed against buffer A [20 mM bis-tris (pH 7.2), 20 mM NaCl, and 10% glycerol] for 12 hours and brought to pH 5.8 by dialyzing against buffer A (pH 5.8) for 30 min. After centrifugation, the dialysate (~650 mg of protein) was loaded onto a Q Sepharose FF column (2.6 cm by 10 cm; Pharmacia), and the column was washed with 120 ml of buffer A (pH 5.8). Proteins were eluted with a 400-ml linear gradient of 20 to 600 mM NaCl in buffer A. Fractions (10 ml; each fraction contained 1 ml of 1 M tris, pH 8, to neutralize the acidic buffer A) were assayed for trapoxin binding activity. Tween-20 was added to active fractions at a final concentration of 0.05%, and these fractions were incubated with K-trap affinity matrix for 16 hours (25 μl per milliliter of Q fraction). After the matrix was washed three times with phosphate-buffered saline, bound proteins were eluted by boiling in 40 μl of SDS sample buffer per 25 μl of matrix. SDS eluates were combined and the proteins resolved by SDS-(PAGE) (12% gel) and transferred to polyvinylidene difluoride membrane (Bio-Rad). Staining with Ponceau S revealed two major bands (46 and 50 kD). The excised bands were proteolytically digested, and the peptide fragments purified by high-performance liquid chromatography were sequenced at the Harvard Microchemistry Facility.
11. Y.-W. Qian *et al.*, *Nature* **364**, 648 (1993).
12. E. J. Neer, C. J. Schmidt, R. Nambudripad, T. F. Smith, *ibid.* **371**, 297 (1994).
13. M. Vidal and R. F. Gaber, *Mol. Cell. Biol.* **11**, 6317 (1991).
14. After noting sequence similarity between peptides derived from the purified bovine trapoxin binding protein and yeast Rpd3p, we checked the dbEST to see whether any partial sequences for the human homolog had been reported. Two ESTs (GenBank accession numbers D31480 and F07807) were identified whose predicted translation products aligned, with sequences similar to the NH_2- and COOH-terminal regions of Rpd3p, respectively. PCR primers were designed on the basis of these tags, and a 1-kb PCR product was obtained from a Jurkat cDNA library (Stratagene). A ^{32}P-labeled probe prepared by random priming was used to screen the Jurkat library, and 10 positive clones were isolated.
15. Control experiments indicated that competitor peptides had no effect on histone deacetylase activity per se (J. Taunton, C. A. Hassig, S. L. Schreiber, unpublished observations).
16. K. Nasmyth, D. J. Stillman, D. Kipling, *Cell* **48**, 579 (1987).
17. D. J. Stillman, S. Dorland, Y. Yu, *Genetics* **136**, 781 (1994).
18. E. A. McKenzie *et al.*, *Mol. Gen. Genet.* **240**, 374 (1993).
19. K. S. Bowdish and A. P. Mitchell, *Mol. Cell. Biol.* **13**, 2172 (1993).
20. L. M. Johnson, P. S. Kayne, E. S. Kahn, M. Grunstein, *Proc. Natl. Acad. Sci. U.S.A.* **87**, 6286 (1990).
21. P. C. Megee, B. A. Morgan, B. A. Mittman, M. M. Smith, *Science* **247**, 841 (1990).
22. E. C. Park and J. W. Szostak, *Mol. Cell. Biol.* **10**, 4932 (1990).
23. O. M. Aparicio, B. L. Billington, D. E. Gottschling, *Cell* **66**, 1279 (1991).
24. M. Braunstein, A. B. Rose, S. G. Holmes, C. D. Allis, J. R. Broach, *Genes Dev.* **7**, 592 (1993).
25. A. Hecht, T. Laroche, S. Strahl Bolsinger, S. M. Gasser, M. Grunstein, *Cell* **80**, 583 (1995).
26. N. A. Clipstone and G. R. Crabtree, *Nature* **357**, 695 (1992).

27. We thank J. L. Collins for preparing [^{3}H]trapoxin; W. S. Lane and colleagues for unparalleled expertise in peptide microsequencing; J. A. Simon for help with molecular biology; K. L. Morrison and L. F. Snow for help with polyclonal antibodies; and Y.-W. Qian and E. Y.-H. Lee for the RbAp48 monoclonal antibody. J.T. extends his gratitude to NSF and Eli Lilly and Co. for predoctoral fellowships. C.A.H. is supported by an NIH predoctoral training grant. S.L.S. is an investigator at the Howard Hughes Medical Institute.

7 December 1995; accepted 27 February 1996

Regulation of an Early Developmental Checkpoint in the B Cell Pathway by Igβ

Shiaoching Gong and Michel C. Nussenzweig*

Many of the cell fate decisions in precursor B cells and more mature B cells are controlled by membrane immunoglobulin (Ig) M heavy chain (mμ) and the Igα-Igβ signal transducers. The role of Igβ in regulating early B cell development was examined in mice that lack Igβ ($Ig\beta^{-/-}$). These mice had a complete block in B cell development at the immature $CD43^+B220^+$ stage. Immunoglobulin heavy chain diversity (D_H) and joining (J_H) segments rearranged, but variable (V_H) to DJ_H recombination and immunoglobulin messenger RNA expression were compromised. These experiments define an unexpected, early requirement for Igβ to produce B cells that can complete VDJ_H recombination.

Membrane immunoglobulins are essential regulatory components in both developing and mature B cells (*1*). Specific events that are controlled by mμ in developing B cells include the precursor B cell (pre–B cell) transition (*2*), allelic exclusion (*3*), receptor editing (*4*), and deletion of lymphocytes that express self-reactive immunoglobulins (*5*). The earliest of these events, allelic exclusion and the pre–B cell transition, are induced by mμ through the mμ-associated Igα-Igβ signal-transducing proteins (*6*). In more mature B cells, the same signal transducers mediate B cell activation by triggering Src and Syk family tyrosine kinases (*7*). All of these mμ-induced cellular responses are thought to be mechanistically related because they share a requirement for phosphorylation of the tyrosine residues in the antigen receptor activation motifs (ARAMs) of the Igα-Igβ complex (*8*).

Howard Hughes Medical Institute, Rockefeller University, New York, NY 10021, USA.

*To whom correspondence should be addressed.

Less is known about the regulation of portions of the B cell pathway that occurs before Ig gene rearrangement. A receptor complex composed of surrogate heavy and light chains, possibly associated with the Igα-Igβ signal transducers, has been proposed as a regulator of these earlier stages of the B cell pathway (*1*, *9*). Support for this hypothesis comes from the observation that Igα and Igβ are expressed when Ig genes are still in the germline configuration (*2*, *10*).

To determine whether the Igα-Igβ complex regulates the early stages of B cell development, we produced a targeted mutation in the mouse Igβ gene (*11*) (Fig. 1). Deletion of the promoter as well as of the first and part of the second coding exons of Igβ resulted in mice that did not express Igβ mRNA (Fig. 2). Northern (RNA) blots with an Igβ complementary DNA (cDNA) probe failed to detect Igβ RNA extracted from bone marrow of $Ig\beta^{-/-}$ mice, whereas a high-intensity signal was present in both wild-type and $RAG\text{-}1^{-/-}$ control RNA samples (Fig. 2). In contrast to Igβ, expres-

sion of Igα mRNA was not affected in Igβ$^{-/-}$ mice (Fig. 2). As in the *RAG-1*$^{-/-}$ mice, the amount of Igα expressed by the Igβ$^{-/-}$ mice was less than that found in wild-type mice but was proportional to the total number of B cells in the sample (Figs. 2 and 3). Thus, Igα continues to be expressed despite the absence of Igβ.

The effects of the Igβ mutation on lymphocyte development in vivo were examined histologically and through the use of fluorescence-activated cell sorting (FACS) analysis. Lymph nodes from mice that lacked Igβ did not develop germinal centers, and spleens had smaller white pulp follicles (Fig. 3; in several experiments, the number of leukocytes in the spleens of Igβ$^{-/-}$ mice was 60% of that found in wild-type littermate controls). Consistent with the lack of germinal centers, Igβ$^{-/-}$ mice had no mature surface μ^{+} peripheral B cells and had a specific block in B cell development in bone marrow (Fig. 3). Analysis of bone marrow cells with antibodies specific for the B220 and CD43 markers revealed that B cell development in Igβ$^{-/-}$ mice progressed to the immature CD43^{+}B220^{+} progenitor B cell (pro–B cell)/pre–BI cell stage [combined fractions A, B, and C in (*12*)]; however, more mature CD43^{-}B220^{+} pre–BII cells (*12*) were completely absent (Fig. 3). Further fractionation with antibodies to the cell surface antigens HSA and BP-1 showed that Igβ$^{-/-}$ mice closely resembled *RAG-1* mutant mice (*2, 12, 13*) (Fig. 3). Consistent with previous observations in *RAG-1* mutant mice, there were no significant differences in the distribution of cells in fractions A, B, and C despite the block in development (*2*). In contrast to the *RAG* mutant mice, the defect in Igβ$^{-/-}$ mice was restricted to the B cell lineage, and T cell development was unaffected (Fig. 3).

The observation that expression of Igα alone failed to induce the pre–B cell transition in Igβ$^{-/-}$ mice differs from the results of experiments with transgenic mice, in which the cytoplasmic domains of Igα and Igβ were each found to be capable of inducing pre–B cell development when expressed as part of chimeric immunoglobulins (*6*). The difference in the two results is likely explained by the documented inability of endogenous Igα to form a homodimeric signaling complex (*14*). Thus, under physiological conditions, progression beyond the CD43^{+}B220^{+} immature B cell stage appears to require the assembly of Igα-Igβ signaling modules.

To further characterize the point in the B cell pathway at which development is interrupted, we assayed for the expression of a series of developmentally regulated B cell–specific mRNAs. Targeting Igβ did not alter the expression of λ5, *RAG-1*, *RAG-2*, Iμ, or μ° and appeared to increase the relative steady-state accumulation of unrearranged V_H mRNAs ($V_H$ster). All of these mRNAs are induced early in the B cell pathway, and the amounts measured suggested that there was no lack of expansion of the pool of early B cell precursors in the Igβ$^{-/-}$ mice (Fig. 2). In contrast, neither Igμ nor Igκ mRNA could be detected in Igβ$^{-/-}$ mice by Northern blotting (Fig. 2). This unexpected result was confirmed by the more sensitive, but less quantitative, reverse transcriptase polymerase chain reaction (RT-PCR) technique, whereby only small amounts of mature Igμ and Igκ mRNAs were found (Fig. 2). We conclude that, in the absence of Igβ, B cell development is interrupted sometime before cells become fully competent to produce Igμ.

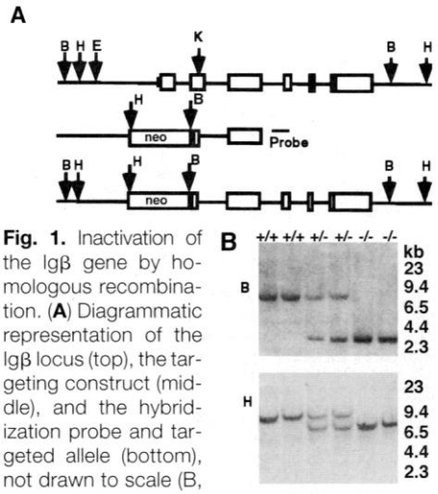

Fig. 1. Inactivation of the Igβ gene by homologous recombination. (**A**) Diagrammatic representation of the Igβ locus (top), the targeting construct (middle), and the hybridization probe and targeted allele (bottom), not drawn to scale (B, Bam HI; H, Hind III; K, Kpn I; E, Eco RV; neo, neomycin). Bam HI and Hind III restriction sites used to detect the targeted gene are indicated. Homologous replacement results in the deletion of a 2-kb region of DNA spanning from the Eco RV site 1 kb upstream of the promoter to the Kpn I site in the middle of the second exon of Igβ; Eco RV and Kpn I sites are indicated (*11, 27*). (**B**) Southern blot of Bam HI– and Hind III–digested tail DNA from pairs of control (+/+), heterozygous (+/−), and homozygous (−/−) Igβ-targeted mice.

Two molecular mechanisms could account for the abnormally low amounts of Ig heavy and light chain mRNAs in Igβ mutant mice. The assembly of fully rearranged Ig transcription units might be defective; alternatively, there could be a specific alteration in the expression of Ig genes. We used PCR to examine Ig gene assembly at the level of D_H to J_H and V_H to DJ_H joining (Fig. 4). Igβ$^{-/-}$ mice had normal levels of D_H to J_H rearrangements, consistent with the expression of sterile μ°, Iμ, *RAG-1*, and *RAG-2* transcripts (*15, 16*) (Fig. 2). Moreover, Dμ mRNAs, the products of D_H to J_H rearrangements, were easily detected by RT-PCR (Fig. 2),

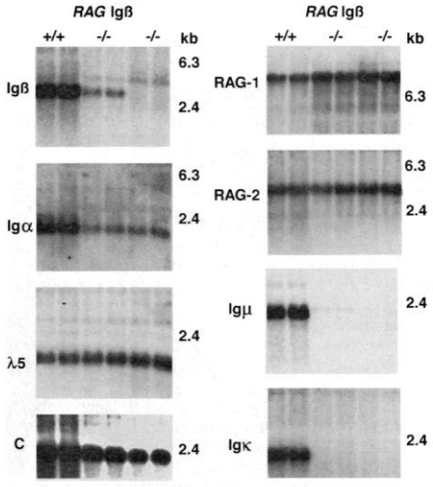

Fig. 2. Expression of developmentally restricted mRNAs in Igβ$^{-/-}$ mice. Northern blot and RT-PCR analysis of bone marrow RNA from 5-week-old Igβ$^{-/-}$ mice, *RAG-1*$^{-/-}$ mice (*RAG*$^{-/-}$), and wild-type littermate controls (+/+) (*28*). The *RAG-1*$^{-/-}$ mice used in these experiments carry an insertion mutation that results in an mRNA that is the same size as *RAG-1* but that does not produce protein (*2*). C, control (GAPDH).

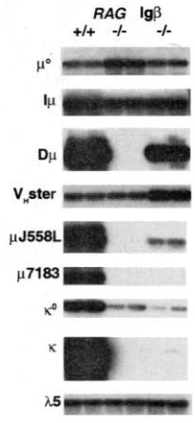

which suggested that fully assembled heavy chain Dμ transcription units are expressed in Igβ$^{-/-}$ pro–B cells. In contrast, the levels of V_H to DJ_H or $V_κ$ to $J_κ$ rearrangements were severely diminished despite a large amount of sterile V_H transcription (Figs. 2 and 4).

To measure the extent of the deficiency in V_H to DJ_H recombination in Igβ$^{-/-}$ mice directly, we examined deletion of the 5′ end of the D_H region in purified CD43^{+}B220^{+} pro–B/pre–BI cells by Southern (DNA) blotting. For this purpose we used a previously characterized probe from the 5′ end of D_H that hybridizes with DNA segments that are normally deleted upon V_H to DJ_H recombination (*17*). An Igμ-CH4 (fourth constant region) probe was included in the hybridization reactions to verify that the amount of DNA was equivalent in each sample. Controls were sorted CD43^{+}B220^{+} B cells [fractions A, B, and C in (*12*)] from *RAG-1* mutant mice, which do not undergo recombination (*13*) [Figs. 3 (gates in top panel) and 4]; wild-type CD43^{+}B220^{+} B cells; and more mature wild-type CD43^{-}B220^{+} B cells.

B cell precursors in Igβ$^{-/-}$ mice closely resembled their *RAG-1*$^{-/-}$ counterparts in

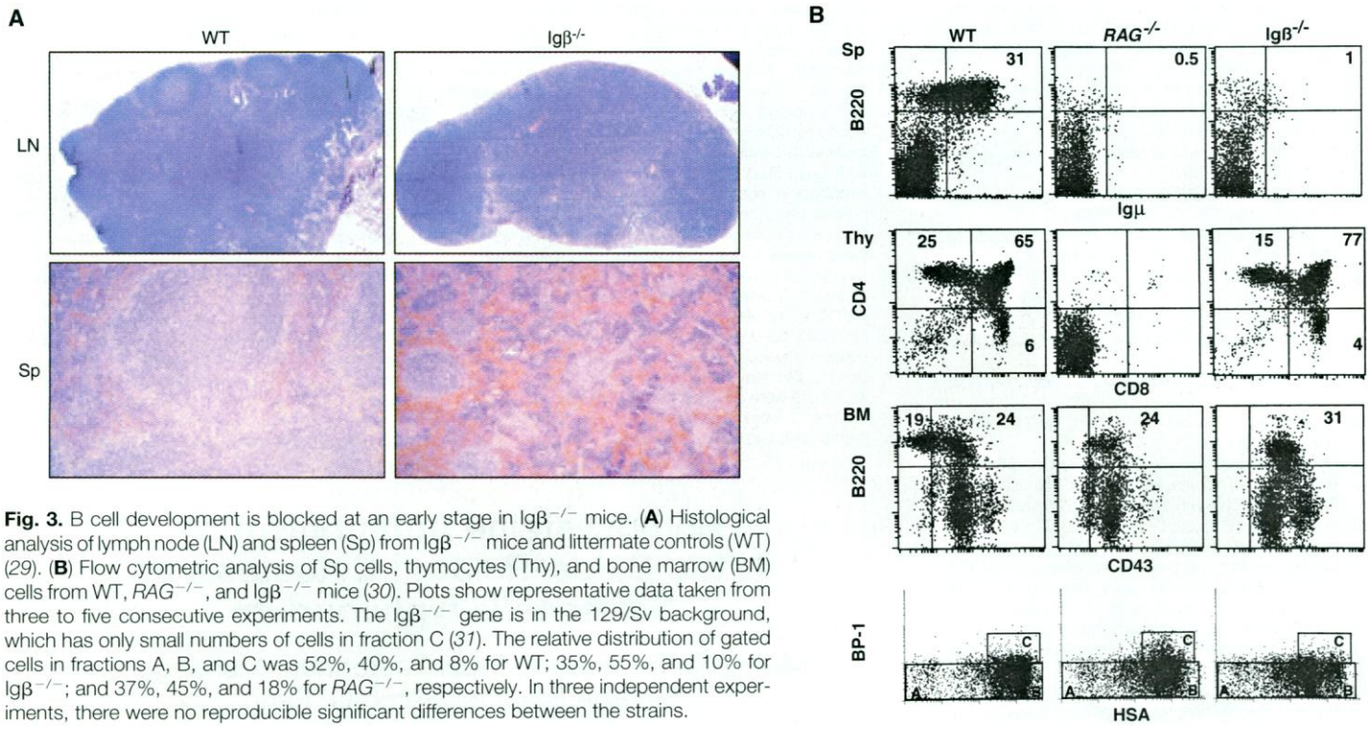

Fig. 3. B cell development is blocked at an early stage in Igβ$^{-/-}$ mice. (**A**) Histological analysis of lymph node (LN) and spleen (Sp) from Igβ$^{-/-}$ mice and littermate controls (WT) (*29*). (**B**) Flow cytometric analysis of Sp cells, thymocytes (Thy), and bone marrow (BM) cells from WT, *RAG*$^{-/-}$, and Igβ$^{-/-}$ mice (*30*). Plots show representative data taken from three to five consecutive experiments. The Igβ$^{-/-}$ gene is in the 129/Sv background, which has only small numbers of cells in fraction C (*31*). The relative distribution of gated cells in fractions A, B, and C was 52%, 40%, and 8% for WT; 35%, 55%, and 10% for Igβ$^{-/-}$; and 37%, 45%, and 18% for *RAG*$^{-/-}$, respectively. In three independent experiments, there were no reproducible significant differences between the strains.

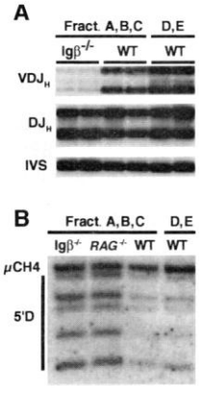

Fig. 4. Immunoglobulin gene rearrangement in Igβ$^{-/-}$ mice. (**A**) Recombination of VJ558L family to DJ_H or of D_H to J_H segments measured by PCR (*16, 24, 32*). DNA samples were extracted from sorted CD43$^+$B220$^+$ and CD43$^+$B220$^-$ bone marrow cells from 5-week-old Igβ$^{-/-}$ mice and WT littermate controls (*33*). (**B**) Southern blot analysis of the extent of V_H to DJ_H rearrangement in purified Igβ$^{-/-}$, *RAG*$^{-/-}$, and WT CD43$^+$B220$^+$, as well as control WT CD43$^-$B220$^+$ bone marrow cells with a probe from the 5′ end of D_H that is deleted upon V_H to DJ_H recombination (*17, 33*). The 5′ end of D_H (5′D) and control Igμ-CH4 (μCH4) hybridizing fragments are indicated. The relative amount of recombination was calculated with a PhosphorImager, with μCH4 hybridization as a loading control and assuming that there was no recombination in the *RAG*$^{-/-}$ B cells as documented previously (*13*) (Fig. 4A). Fract., fractions.

that little of the 5′ D_H segment deletion could be detected (Fig. 4). By PhosphorImager analysis, only 9% of the V_H alleles in CD43$^+$B220$^+$ B cells from Igβ$^{-/-}$ mice had rearranged. In contrast, 60% of the V_H alleles were rearranged in comparably sorted wild-type CD43$^+$B220$^+$ B cells (Figs. 3B and 4). We conclude that in the absence of Igβ, B cells are predominantly trapped in a stage that has been variously referred to as the null pre-B, pre-BI, or early pre-B stage (*1*, *17*). This is in contrast to the phenotype observed when the transmembrane domain of Igμ is disrupted (μMT$^{-/-}$) (*18*). μMT$^{-/-}$ B cells cannot produce mμ and therefore do not assemble a mμ-Igα-Igβ complex [precursor B cell receptor (pre-BCR)]. Despite the lack of a pre-BCR in μMT$^{-/-}$ mice, CD43$^+$B220$^+$ pre–B cells accumulate normal numbers of V_H to DJ_H joints (*18*). Thus, the absence of mμ allows development to proceed to a stage that is competent for V_H to DJ_H joining, whereas the absence of Igβ results in B cells that fail to progress beyond D_H to J_H recombination despite high amounts of expression of *RAG-1*, *RAG-2*, sterile V_H, I_μ, and μ°. The finding that transcription of *RAG-1*, *RAG-2*, and sterile μ is sufficient for D_H to J_H but not V_H to DJ_H joining is in agreement with experiments with transgenic recombination substrates (*19*). Together, these genetic experiments strongly support a mμ-independent role for Igβ in regulating B cell development.

Pre–BI cells are found in human tumors and can be isolated by Abelson virus transformation of fetal liver cells (*17*) or by cell sorting (*1*). In tissue culture, maintenance of the pre–BI phenotype is dependent on interleukin 7 and contact with bone marrow feeder cells (*20*). However, the physiological signal that normally activates progression to the pre–BII stage has not been defined. The finding that Igβ is required for regulation of this important checkpoint is consistent with a function for the Igα-Igβ signal transducer in B cell development that is earlier than suspected, possibly working in conjunction with a proposed surrogate heavy and light chain complex (*9*, *21*).

REFERENCES AND NOTES

1. D. Loffert *et al.*, *Immunol. Rev.* **137**, 135 (1994); A. Rolink and F. Melchers, *Cell* **66**, 1081 (1991).
2. E. Spanopoulou *et al.*, *Genes Dev.* **8**, 1030 (1994); F. Young, *ibid.*, p. 1043.
3. M. C. Nussenzweig *et al.*, *Science* **236**, 816 (1987); J. Manz, K. Denis, O. Witte, R. Brinster, U. Storb, *J. Exp. Med.* **168**, 1363 (1988); D. Kitamura and K. Rajewsky, *Nature* **356**, 154 (1992).
4. S. L. Tiegs, D. M. Russell, D. Nemazee, *J. Exp. Med.* **177**, 1009 (1993); M. Z. Radic, J. Erickson, S. Litwin, M. Weigert, *ibid.*, p. 1165.
5. D. A. Nemazee and K. Bürki, *Nature* **337**, 562 (1989); S. B. Hartley *et al.*, *ibid.* **353**, 765 (1991); C. Chen *et al.*, *ibid.* **373**, 252 (1995); M. Okamoto *et al.*, *J. Exp. Med.* **175**, 71 (1992).
6. F. Papavasiliou, Z. Misulovin, H. Suh, M. C. Nussenzweig, *Science* **268**, 408 (1995); F. Papavasiliou, M. Jankovic, H. Suh, M. C. Nussenzweig, *J. Exp. Med.* **182**, 1389 (1995).
7. M. R. Gold and A. L. DeFranco, *Adv. Immunol.* **55**, 221 (1994); C. M. Pleiman, D. D'Ambrosio, J. C. Cambier, *Immunol. Today* **15**, 393 (1994); M. Reth, *Curr. Opin. Immunol.* **6**, 3 (1994).
8. M. Reth, *Nature* **338**, 383 (1989).
9. H. Karasuyama, A. Rolink, F. Melchers, *J. Exp. Med.* **178**, 469 (1993).
10. Y. Zhuang, P. Soriano, H. Weintraub, *Cell* **79**, 875 (1995); G. Bain *et al.*, *ibid.*, p. 885; X.-H. Sun, *ibid.*, p. 893; P. Urbanek, Z.-Q. Wang, I. Fetka, E. F. Wagner, M. Busslinger, *ibid.*, p. 901; H. Lin and R. Grosschedl, *Nature* **376**, 263 (1995).
11. G. G. Hermanson, D. Eisenberg, P. W. Kincade, R. Wall, *Proc. Natl. Acad. Sci. U.S.A.* **85**, 6890 (1988).
12. R. R. Hardy, C. E. Carmack, S. A. Shinton, J. D. Kemp, K. Hayakawa, *J. Exp. Med.* **173**, 1213 (1991).
13. P. Mombaerts *et al.*, *Cell* **68**, 869 (1992); Y. Shinkai *et al.*, *ibid.*, p. 855.
14. J. Hombach, T. Tsubata, L. Leclercq, H. Stappert, M. Reth, *Nature* **343**, 760 (1990); T. E. Costa, R. R.

Franke, M. Sanchez, Z. Misulovin, M. C. Nussenzweig, *J. Exp. Med.* **175**, 1669 (1992); A. R. Venkitaraman, G. T. Williams, P. Dariavach, M. S. Neuberger, *Nature* **352**, 777 (1991).
15. G. G. Lennon and R. P. Perry, *Nature* **318**, 475 (1985); F. W. Alt, T. K. Blackwell, G. D. Yancopoulos, *Science* **238**, 1079 (1987).
16. M. S. Schlissel, L. M. Corcoran, D. Baltimore, *J. Exp. Med.* **173**, 711 (1991).
17. F. W. Alt *et al.*, *EMBO J.* **3**, 1209 (1984).
18. A. Ehlich *et al.*, *Cell* **72**, 695 (1993).
19. P. Ferrier *et al.*, *EMBO J.* **9**, 117 (1990); A. Okada, M. Mendelsohn, F. Alt, *J. Exp. Med.* **180**, 261 (1994).
20. U. Grawunder, D. Haasner, F. Melchers, *Int. Immunol.* **5**, 1609 (1993).
21. H. Karasuyama *et al.*, *Cell* **77**, 133 (1994).
22. P. J. Swiatek and T. Gridley, *Genes Dev.* **7**, 2071 (1993).
23. D. A. Melton *et al.*, *Nucleic Acids Res.* **12**, 7035 (1984).
24. A. Kudo, N. Sakaguchi, F. Melchers, *EMBO J.* **6**, 103 (1987).
25. M. S. Schlissel and D. Baltimore, *Cell* **58**, 1001 (1989); T. E. F. Costa, H. Suh, M. C. Nussenzweig, *Proc. Natl. Acad. Sci. U.S.A.* **89**, 2205 (1992).
26. H. P. Petree, F. Livak, D. Burtrum, S. Mazel, *J. Exp. Med.* **182**, 121 (1995).
27. Murine genomic Igβ DNA clones were isolated from a 129/Sv strain genomic library. The long arm of the targeting vector consisted of 10 kilobases (kb) of DNA 5′ to the Eco RV site, which is 1 kb upstream of the Igβ promoter. The short arm was a 1.2-kb fragment from the Kpn I site in the second exon to the Xba I site in the third intron. Homologous insertion resulted in a deletion of the promoter, the first exon, and the portion of the second exon that is 5′ to the Kpn I site. The targeting construct was linearized with Not I and transfected into CJ7 (*22*) embryonic stem (ES) cells. Two hundred ES cell clones were screened, and four clones carrying the mutation in Igβ were identified by Southern blotting. All four were injected into C57Bl/6 blastocysts, and three of the four clones produced chimeric mice that transmitted the mutation.
28. For Northern blotting, 2 μg of total RNA was run on denaturing formaldehyde-agarose gels and transferred to nylon membranes. Filters were probed with reverse RNA probes (*23*). Glyceraldehyde-3-phosphate dehydrogenase (GAPDH) was used as a loading control. For RT-PCR experiments, total RNA was first digested with deoxyribonuclease (DNAse) and then reverse-transcribed (*16*). Amounts of cDNA were normalized to GAPDH and λ5 (see Fig. 2). Amplification conditions were as follows: 30 cycles of 1 min at 94°C, 1 min at 60°C, and 1.75 min at 72°C, followed by a single 10-min period at 72°C. PCR products were electrophoresed on agarose gels, transferred to nylon membranes, and probed with the following specific DNA probes: (i) Hind III–Bgl I fragment from the mouse Cκ region for κ° and κ; (ii) Eco RI fragment covering mouse μCH1 for μJ558L, μ7183, Dμ, μ°, and Iμ; (iii) mouse λ5 cDNA for λ5 (*24*); and (iv) V_HJ558L for $V_H$ster. The PCR primers for μ°, Iμ, Dμ, μJ558L, μ7183, κ°, κ, λ5, and $V_H$ster were as described previously (*10, 16, 25*).
29. Lymph nodes and spleens were photographed at magnifications of ×10 and ×25, respectively. Tissues from 5-week-old mice were fixed with formalin, and tissue sections were stained with hematoxylin and eosin.
30. For two-color analysis, single-cell suspensions from lymphoid organs of 5-week-old mutant and littermate control mice were prepared for staining as described previously and analyzed on a Becton Dickinson FACScan with CELLQuest software (*6*). Bone marrow cells (yield, 1.5×10^7 to 2×10^7 cells per mouse for all strains) were stained with phycoerythrin (PE)–labeled antibody to B220 and fluorescein isothiocyanate (FITC)–labeled antibody to CD43, spleen cells (yield, 6×10^7 to 7×10^7 for $Igβ^{-/-}$ mice and 10^8 for wild-type mice) were stained with FITC-labeled antibody to μ and PE-labeled antibody to B220, and thymocytes (yield, 10^8 for both $Igβ^{-/-}$ mice and wild-type controls) were stained with PE-labeled antibody to CD4 and FITC-labeled antibody to CD8 (Pharmingen). Gating was based on lymphocyte scatter; 5000 to 10,000 gated events are shown in each panel. For four-color analysis, bone marrow cells were stained simultaneously with allophycocyanin (APC)-labeled antibody to B220, FITC-labeled antibody to CD43, PE-labeled antibody to HSA, and biotinylated antibody to BP-1. BP-1 was visualized with Texas Red avidin (Pharmingen). Gating was on lymphocyte scatter and then on $CD43^+B220^+$ cells as described (*12*). Ten thousand events taken from the $CD43^+B220^+$ gate are shown in each panel. Analysis was on a FACstar-plus system with the Lysis-II program (Becton Dickinson).
31. A. Ehlich, V. Martin, W. Muller, K. Rajewsky, *Curr. Biol.* **4**, 573 (1994).
32. For PCR, bone marrow DNA was amplified as described previously (*16, 24*). VJ558L primers were used for the heavy chain in this experiment, but similar results were also seen with V7183 primers. PCR fragments were visualized after transfer to nylon membranes by probing with an Eco RI fragment that covers the mouse J_H region (V-DJ_H and D_H-J_H). The two bands detected correspond to D_H-J_H1 and 2 and V-DJ_H1 and 2, respectively. Control primers were from the J-CH1 intervening sequence (IVS) (*24*).
33. For Southern blotting, B cells were purified from bone marrow by sorting $CD43^+B220^+$ and $CD43^+B220^-$ cells (*12*). The gates were set with *RAG-1*$^{-/-}$ $CD43^+B220^+$ control cells. The sorted cells were processed to make DNA for restriction enzyme digestion in agarose, as described (*26*). DNA samples were digested with Pst I, separated on agarose gels, transferred to nylon membranes, and probed with a combination of a 700–base pair Pst I–Pst I probe from the 5′ end of D_H (*17*) and a 650-bp Hind III–Pst I fragment that covers Igμ-CH4.
34. We thank M. Sanchez and T. Dlohery for the FACS analyses; K. Sokol for histology; H. Petree, A. Fienberg, X. Qin, and Z. Misulovin for technical advice; and S. Gezelter and F. Isdell for cell sorting.

13 October 1995; accepted 7 February 1996

Homocysteine Antagonism of Nitric Oxide–Related Cytostasis in *Salmonella typhimurium*

Mary Ann De Groote, Traci Testerman, Yisheng Xu, George Stauffer, Ferric C. Fang*

Nitric oxide (NO) is associated with broad-spectrum antimicrobial activity of particular importance in infections caused by intracellular pathogens. An insertion mutation in the *metL* gene of *Salmonella typhimurium* conferred specific hypersusceptibility to *S*-nitrosothiol NO-donor compounds and attenuated virulence of the organism in mice. The *metL* gene product catalyzes two proximal metabolic steps required for homocysteine biosynthesis. *S*-Nitrosothiol resistance was restored by exogenous homocysteine or introduction of the *metL* gene on a plasmid. Measurement of expression of the homocysteine-sensitive *metH* gene indicated that *S*-nitrosothiols may directly deplete intracellular homocysteine. Homocysteine may act as an endogenous NO antagonist in diverse processes including infection, atherosclerosis, and neurologic disease.

Nitric oxide has antimicrobial activity against a broad array of pathogens ranging from viruses to helminths (*1*), but the specific reactive nitrogen intermediates responsible for this activity are undetermined. *S*-Nitrosothiols such as *S*-nitrosoglutathione (GSNO) are candidate endogenous antimicrobial mediators because they have broad-spectrum microbiostatic activity (*2, 3*) and have been detected during inflammatory states in vivo (*4*). Although *S*-nitrosothiols can function as NO^- donors, observations in the Gram-negative bacterium *Salmonella typhimurium* suggest that their cytostatic activity actually results from NO^+ (nitrosonium) transfer after active transport of the *S*-nitrosothiol into the target cell (*2*). *Salmonella* provides a model system in which to examine the antimicrobial properties of NO because it is genetically well characterized (*5*), resides principally within host cells (*6*), and requires host expression of NO-stimulatory cytokines for effective clearance (*7*).

A *S. typhimurium* MudJ (*8*) transposon library was enriched for mutants hypersusceptible to *S*-nitrosothiols by simultaneous exposure to cycloserine and subinhibitory concentrations of GSNO (*9*). A clone highly susceptible to GSNO and other nitrosothiols was found to harbor an insertion in the *metL* gene (*10*), encoding the bifunctional enzyme aspartokinase II–homoserine dehydrogenase II (AKII-HDII). The *metL* mutant strain was designated *S. typhimurium* MF1000. AKII-HDII catalyzes two independent proximal steps in the prokaryotic biosynthetic pathways that convert aspartate to lysine, threonine, and methionine (Fig. 1). The increased susceptibility conferred by the *metL* mutation appears to be specific for *S*-nitrosothiols, because no marked effect on susceptibility to the per-

M. A. De Groote, T. Testerman, Y. Xu, F. C. Fang, Departments of Medicine, Pathology, and Microbiology, University of Colorado Health Sciences Center, Denver, CO 80262, USA.
G. Stauffer, Department of Microbiology, University of Iowa, Iowa City, IA 52242, USA.
*To whom correspondence should be addressed.